Ultraviolet emission from porous silicon photosynthesized in aqueous alkali fluoride solutions

Kaoru Uchida, Katsuhiro Tomioka, and Sadao Adachi[a)]
Department of Electronic Engineering, Faculty of Engineering, Gunma University, Kiryu-shi, Gunma 376-8515, Japan

(Received 17 November 2005; accepted 18 April 2006; published online 6 July 2006)

Stable ultraviolet (UV) photoluminescence (PL) has been observed at room temperature in porous silicon (PSi) fabricated by photoetching in aqueous alkali fluoride solutions. The aqueous solutions used are 1 *M* NaF and 1 *M* KF. They give an alkaline reaction caused by partial hydrolysis. The PL peaks at ~3.3 eV have a full width at half maximum of ~0.1 eV, which is much smaller than those reported previously (≥0.5 eV). Spectral analyses suggest that both quantum confinement and surface passivation effects enable the observation of UV emission in NaF- and KF-prepared PSi samples. © *2006 American Institute of Physics*. [DOI: 10.1063/1.2208914]

I. INTRODUCTION

Many studies have been carried out on porous silicon (PSi), because it shows not only efficient photoluminescence (PL) but also injection-type electroluminescence in the visible region at room temperature.[1,2] Most light-emitting PSi layers are prepared by conventional anodic etching. Aluminum is evaporated on the back surface of a *p*-type silicon wafer for use as the Ohmic back contact. Anodic etching is then performed in an aqueous HF solution or an ethanol/HF solution with an applied electrical bias. The requirement for a back-contact electrode and electronic circuits is a weakness of the anodic etching.

To overcome this, several authors[3–7] carried out the stain etching of silicon wafers in HF/HNO_3-based solutions and fabricated PSi layers similar to those obtained by anodic etching. All the layers obtained emitted light in the red spectral region. The photoetching of silicon in aqueous HF solution[8,9] or a HF/H_2O_2 solution mixture[10,11] under He–Ne laser illumination has also been proposed. Such photosynthesized PSi showed a red[8,9] or yellow emission at room temperature.[10,11]

We have recently shown that an aqueous NaF or KF solution causes the removal of the native oxide on a silicon wafer immersed in it at room light.[12,13] Note that these solutions are less toxic and easier to handle than HF. Indeed, NaF is commonly used in dental clinics for the prevention of tooth decay. The etching rate of the native oxide was determined to be ~0.02–0.05 nm/min.[12,13] X-ray photoelectron spectroscopy suggested that NaF- and KF-treated silicon surfaces are as clean as silicon surfaces etched in a HF solution. An as-degreased silicon surface is hydrophilic (contact angle: $\theta \sim 35°$), whereas silicon surfaces cleaned in NaF and KF solutions are hydrophobic ($\theta \sim 70° - 80°$).

The purpose of this study is to show that the photoetching of silicon in aqueous alkali fluoride solutions enables the fabrication of light-emitting PSi in the ultraviolet (UV) spectral region. The fabricated PSi emits light at ~3.3 eV with a full width at half maximum (FWHM) of ~0.1 eV.[14] For comparison, photosynthesized PSi in aqueous HF solution is also prepared. Atomic force microscopy (AFM) and Fourier transform infrared (FTIR) spectroscopy are used to assess the surface morphology and chemistry of photosynthesized PSi samples. Chemical dissociation and the mechanism of UV emission in such photosynthesized PSi are discussed. The preliminary result of long-term PL emission stability is presented.

II. EXPERIMENT

The wafers used in this study were *n*-type Si(111) with a resistivity range of 13–20 Ω cm. They were first degreased using organic solvents in an ultrasonic bath, rinsed in deionized (DI) water, etched in 46% HF solution for 1 min, and finally rinsed in DI water. Photochemical etching was performed by illuminating a 5 mW He–Ne laser ($\lambda = 632.8$ nm) onto the sample surface in 1 *M* NaF or 1 *M* KF solution for 3 h. The *p*H range of these solutions was ~7.3–7.5. The laser beam was expanded to approximately 1.5–2 mm in diameter. For comparison, we fabricated a PSi sample using the same method, but immersed in 23% (12.5 *M*) HF solution for 3 h. After photoetching, the samples were rinsed in DI water.

The surface morphology of the PSi samples was determined by *ex situ* AFM, using Digital Instruments Nanoscope III. AFM images were acquired in the tapping mode and repulsive force regime with a contact force on the ~1 nN order between the cantilever and sample surface. PL measurement was performed using a grating spectrometer (Jasco CT-25C) and a Peltier-device-cooled photomultiplier tube (Hamamatsu R375). The 325 nm line of a He–Cd laser (Kimmon IK3302R-E) chopped at 328 Hz was used as the excitation light source. The surface chemistry of the PSi samples was examined by FTIR spectroscopy. FTIR spectra were recorded using a Nicolet Magna 560 spectrometer in the 400–4000 cm^{-1} region at a resolution of 8 cm^{-1}.

a)Electronic mail: adachi@el.gunma-u.ac.jp

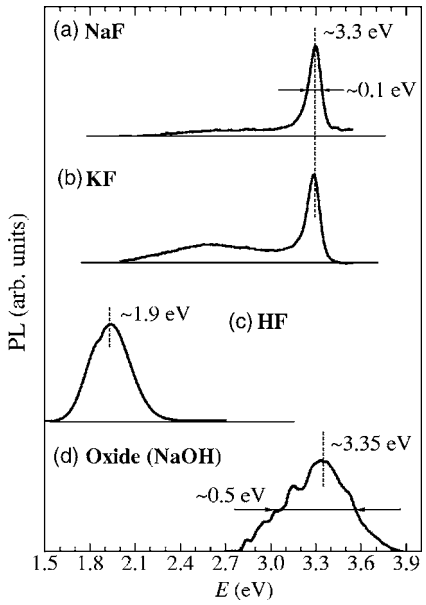

FIG. 1. Room-temperature PL spectra of PSi photosynthesized in (a) 1 *M* NaF, (b) 1 *M* KF, and (c) 23% HF solutions for 3 h, together with that of (d) anodically deposited oxide film on silicon in ~40% NaOH solution (Ref. 15).

III. RESULTS

A. PL measurement

Figure 1 shows the room-temperature PL spectra of PSi samples prepared in (a) 1 *M* NaF and (b) 1 *M* KF solutions, together with that prepared in (c) 23% HF solution. The HF-prepared PSi sample exhibits a very broad emission band at ~1.9 eV, which is typically observed in PSi fabricated by electrochemical or stain etching in HF-based solutions.[1,2] On the other hand, the NaF- and KF-prepared PSi samples show a distinct UV peak at ~3.3 eV, together with a broad emission band peaking at ~2.6–2.7 eV. The UV peaks observed at ~3.3 eV in the NaF- and KF-prepared samples are very narrow, yielding a FWHM of ~0.1 eV.

Recently, Yang *et al.*[15] have observed UV emission from an anodic film deposited on silicon in 40 wt % NaOH solution at a current density of 30 mA/cm^2 for 30 min. We reproduce in Fig. 1(d) their obtained PL spectrum.[15] We can see that the anodic film shows a broad peak at ~3.35 eV with a FWHM of ~0.5 eV. Such a broad UV emission band has been typically observed in silicon-based porous materials.[16–19]

B. AFM image

The quantum confinement model explained visible luminescence from PSi. Afterwards, many other alternative models have been proposed.[1,2] Except for the quantum confinement model, all the others assume an extrinsic origin of PSi luminescence. To determine whether the UV emission observed in the NaF- and KF-prepared PSi samples is due to quantum confinement effects, we used *ex situ* AFM. Figure 2 shows large-scale AFM images of the PSi samples prepared in 1 *M* NaF [Fig. 2(b)], 1 *M* KF [Fig. 2(c)], and 23% HF [Fig. 2(d)] solutions. For comparison, an AFM image of a Si(111) surface immersed in 1 *M* NaF solution for 3 h without light illumination is shown in Fig. 2(a).

The AFM images in Figs. 2(b)–2(d) reveal many irregularly shaped pores and voids distributed randomly over the entire surface. The rms roughnesses obtained from these images are 3.4 nm [Fig. 2(b)], 3.2 nm [Fig. 2(c)], and 3.6 nm [Fig. 2(d)]. The lateral microstructure sizes in Figs. 2(b)–2(d)

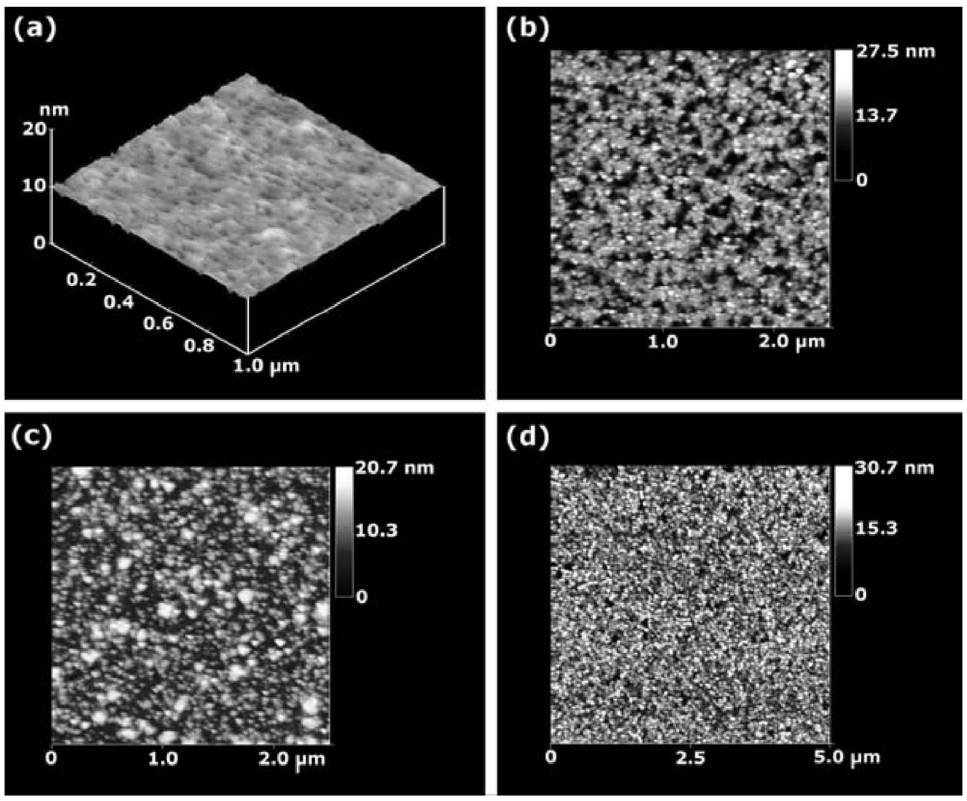

FIG. 2. Large-scale AFM images of (a) Si(111) wafer immersed in 1 *M* NaF solution for 3 h in the dark, (b) PSi photosynthesized in 1 *M* NaF solution for 3 h, (c) PSi photosynthesized in 1 *M* KF solution for 3 h, and (d) PSi photosynthesized in 23% HF solution for 3 h. The rms roughnesses obtained are (a) ~0.2, (b) 3.4, (c) 3.2, and (d) 3.6 nm, respectively.

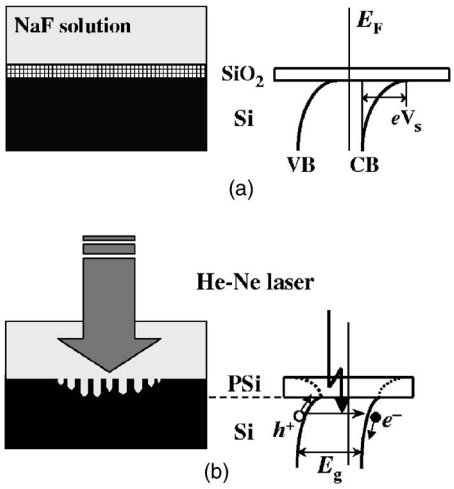

FIG. 3. Schematic energy band structure at NaF solution/silicon interface (a) immediately after immersing silicon wafer in NaF solution and (b) after photoetching in NaF solution under He–Ne laser illumination. CB =conduction band; VB=valence band; E_F=Fermi energy; eV_s=band bending; and E_g=band-gap energy.

are also found to be in the range of 20–50 nm. On the other hand, the rms roughness of the sample immersed in the 1 *M* NaF solution without light illumination is ~0.2 nm [Fig. 2(a)], which is comparable to those of polished, HF-etched Si(111) wafers measured by scanning tunneling microscopy (0.12–0.18 nm).[20] No PL emission was observed from such shiny flat sample surfaces prepared without light illumination.

The lack of a clear difference in lateral sizes between the alkali-fluoride-prepared and HF-prepared PSi samples suggests that the strong UV emission observed only in the alkali-fluoride-prepared samples is not due to quantum size effects. Note, however, that a careful study is needed to detect nanocrystalline size as small as 3 nm. Indeed, the AFM rms roughness and lateral microstructure size obtained by Vinod and Lal[21] for anodic PSi in ethanolic HF solution were 2.5–5 and ~80 nm, respectively. It is very hard to expect UV (or visible) emission from such PSi samples with lateral microstructure sizes as large as 20–80 nm as observed by AFM (Fig. 2 and Ref. 21). A transmission electron microscopy (TEM) image of anodized PSi (Ref. 2 and 22) showed undulating silicon columns with diameters less than 3 nm that were crystalline in nature. For stain-etched PSi samples,[6] the dimensions of most pits were on the order of ~2000–4000 Å, which are much larger than the sizes required to induce quantum confinement effects. However, a careful comparison with a micrograph of a conventionally anodized sample revealed that the surface morphologies are similar, suggesting that the stain etching can produce a light-emitting PSi layer on the surface.[4,6] Furthermore, the AFM and TEM of conventionally anodized, laterally anodized, and stain-etched silicon layers showed that these porous layers have a "fractal-type" surface morphology.[23]

The schematic energy band configurations in the vicinity of the surface of a *n*-type silicon before and after photoetching in 1 *M* NaF solution are shown in Fig. 3. Note that the use of an aqueous NaF solution resulted in an alkaline reaction induced by partial hydrolysis:

$$NaF_{(s)} + H_2O_{(l)} \rightarrow Na^+_{(aq)} + OH^-_{(aq)} + HF_{(aq)}. \quad (1)$$

HF in Eq. (1) can be used to etch-remove the native oxide film on a Si(111) surface:

$$SiO_{2(s)} + 4HF_{(aq)} \rightarrow SiF_{4(aq)} + 2H_2O_{(l)}. \quad (2)$$

The etching rate of the native silicon oxide in 1 *M* NaF solution was determined to be ~0.02 nm/min.[12]

The illumination of a He–Ne laser produces free electron (e^-)-hole (h^+) pairs in the silicon substrate, as shown in Fig. 3(b). Photoexcited carriers are then separated by the electric field in the surface space-charge layer, with electrons and holes drifting into opposite directions. Excess minority holes in *n*-type silicon that move toward the surface may lead to the redistribution of the equilibrium space charge and consequently to a decrease in the degree of band bending eV_s. The existence of a broad range of silicon pore sizes results in the distribution of the PSi band-gap energy, as schematically illustrated in Fig. 3(b) by dashed lines.

In anodic etching, as porous silicon is formed, hydrogen gas is evolved at the electrode surface. This is also the case in photoetching. This dissolution reaction can be written as [24]

$$Si_{(s)} + 6HF_{(aq)} + xh^+ \rightarrow SiF^{2-}_{6(aq)} + (6-2y)H^+_{(aq)} + yH_{2(g)} + ze^-, \quad (3)$$

where $x+2y+z=4$. Note that the above reaction can be expected in both aqueous NaF and HF solutions. Equation (3) supports the hypothesis that the oxidation of a surface silicon atom occurs via three routes: (i) hole capture, (ii) electron injection, and (iii) hydrogen evolution.

OH^- in Eq. (1) enables another etching mechanism, i.e., an alkaline etching of silicon written as

$$Si_{(s)} + 2OH^-_{(aq)} + 2H_2O_{(l)} \rightarrow SiO_2(OH)^{2-}_{2(aq)} + 2H_{2(g)}. \quad (4)$$

Hydrogen is evolved during silicon etching in alkaline solutions (e.g., NaOH and KOH).[25]

C. FTIR spectroscopy

Yang *et al.*[15] suggested that the UV (~3.35 eV) emission observed in Fig. 1(d) occurs at the interface between bulk silicon and its oxide, which is closely associated with a characteristic infrared absorption band at ~1250 cm^{-3}. This characteristic band may originate from the "$-SiO_3$" group, which bonds to the silicon surface structure. Finally, the ~1250 cm^{-3} absorption band is considered to be a good indicator of UV emission in silicon-based nanostructured materials.[15]

To further analyze our PSi samples, we performed FTIR spectroscopy at room temperature. Figure 4 shows FTIR spectra of (a) as-degreased silicon, (b) HF-prepared PSi, and (c) KF-prepared PSi, together with that of (d) UV-emitting oxide film deposited anodically on bulk silicon in ~40% NaOH solution (Ref. 15).

The FTIR spectrum of the as-degreased silicon [Fig. 4(a)] exhibits strong absorption bands near 613 and ~1107 cm^{-1}. The most distinct peak at ~613 cm^{-1} can be assigned to the summation band of the transverse optical (TO) and transverse acoustic (TA) phonons at the

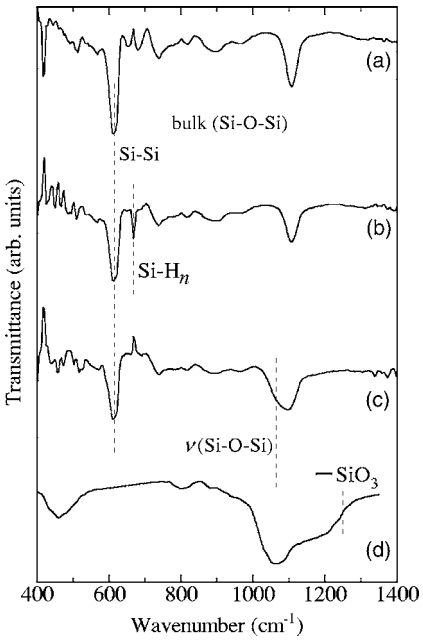

FIG. 4. FTIR spectra of (a) as-degreased silicon, (b) red-emitting PSi prepared by photoetching in 23% HF solution, (c) UV-emitting PSi prepared by photoetching in 1 *M* KF solution, and (d) UV-emitting oxide film deposited anodically on bulk silicon in ~40% NaOH solution (Ref. 15).

X(610.6 cm^{-1}) or L(603.9 cm^{-1}) point.[26] The distinct peak at ~1107 cm^{-1} may also be due to a multiphonon band.[26] Note, however, that the 1040–1240 cm^{-1} spectral region is largely obscured by residual impurities. In fact, the relatively distinct peak observed at ~1107 cm^{-1} has been assigned to the bulk Si–O–Si mode.[27,28] The distinct peak observed at ~668 cm^{-1} in the FTIR spectrum of HF-prepared PSi [Fig. 4(b)] can be assigned to the Si–H_n wagging vibration of SiH_2 surface species.[29]

The significant difference in FTIR spectra between HF-prepared PSi [Fig. 4(b)] and KF-prepared PSi [Fig. 4(c)] is the new absorption peak near the bulk Si–O–Si peak at ~1107 cm^{-1}. This new absorption peak is observed at ~1065 cm^{-1} and is assigned to the surface Si–O–Si stretching mode ν(Si–O–Si).[28]

We also performed the passive etching of KF-prepared PSi in HF solution and found that the ~3.3 eV emission peak disappears, whereas the red-emission peak grows at ~1.95 eV.[14] This etching led to the removal of the surface ν(Si–O–Si) stretching peak at ~1065 cm^{-1}. The resultant PL and FTIR spectra resembled those of photosynthesized PSi in aqueous HF solution. These results support the notion that a thin surface oxide layer (~1065 cm^{-1}) is necessary in observing strong UV emission from PSi samples.

On the other hand, the anodic oxide film deposited in NaOH solution displays three typical Si–O–Si rocking and stretching vibration bands at ~460, 800, and 1070 cm^{-1}, together with an additional absorption band at ~1250 cm^{-1} [Fig. 4(d)]. Yang *et al.*[15] found that this additional band is frequently observed in oxidized PSi and silicon oxide films, usually accompanied with an UV emission peak [see Fig. 1(d)]. They concluded that the broad UV emission at ~370 nm (~3.35 eV) originates from the "–SiO_3" group, which bonds to the silicon structural surface.

IV. DISCUSSION

Several authors have reported UV emission in PL spectra of porous silicon.[16–19] Qin *et al.*.[16] studied thermally oxidized anodic PSi samples and observed almost the same UV emissions as those seen in the PL spectrum of SiO_2 powders. They concluded that the luminescence centers in silicon oxide are responsible for UV emission in both PSi and SiO_2 powders. Mizuno *et al.*[17] also observed UV emission from anodic and subsequently photo-oxidized PSi in an ethanolic HF solution under the open-circuit condition. After photo-oxidation, the PL emission shifted from red (~1.8 eV) to blue (~3.1 eV), with a decrease in its strength from 1 to approximately 1/200. Mizuno *et al.* considered that the blue-shift in the PL spectrum is promoted by photochemical etching and by a consequent size reduction of the silicon crystallite. On the other hand, Wolkin *et al.*[18] demonstrated that the PL of silicon quantum dots present in PSi can be tuned from near infrared to ultraviolet when the surface is passivated with Si–H bonds. After exposure to oxygen, the PL spectrum shifted to red by as much as 1 eV. They concluded that both quantum confinement and surface passivation determine the electronic states of silicon quantum dots.

More recently, Chen *et al.*[19] observed a strong, stable UV emission at ~3.4 eV in manganese-passivated PSi prepared by the hydrothermal technique. The Mn-passivated silicon nanocrystallite was considered to consist of three regions: the core, interfacial (the OH group and Mn^{2+} ion co-passivation of silicon dangling bonds), and outer MnO_2 layer. Note that all these UV emission bands reported in Refs. 16–19 had a FWHM $\geqslant$0.5 eV. Strong UV emissions at ~3.7–3.8 eV have also been observed in porous silica samples;[30,31] however, their spectral widths $\geqslant$0.5 eV are also much larger than that observed in this study (~0.1 eV).

The very narrow spectral width observed in our alkali-fluoride-prepared PSi samples suggests that the origin of this emission is very unique. We can, however, omit the possibility of silica being the origin. This is because no strong silica absorption band was observed in our FTIR spectra at ~460, 800, or 1100 cm^{-1}. Note that the bulk Si–O–Si peak observed at ~1107 cm^{-1} in Figs. 4(a)–4(c) is due to surface native oxide, where its thickness is determined to be ~1–2 nm or less.[12,13] This is in direct contrast to the case of the heavily oxidized PSi layer in Fig. 4(d). The weaker absorption peak ν(Si–O–Si) at ~1065 cm^{-1} in Fig. 4(c) may support the result that its volume or layer thickness is too small to produce an efficient PL emission. Thus, we omit the possibility of the ~3.3 eV emission arising from silica or silicon oxide. Yamamoto and Takai[32] also observed the relatively distinct ν(Si–O–Si) peak in a blue-emitting PSi layer fabricated by photoetching in a HF/H_2O_2 solution and the subsequent dipping in an ethanol/H_2O solution for 148 h, and concluded that their observed blue emission is caused by the oxidized porous layer.

It is possible that our observed UV emission is caused by the effects of quantum confinement. The smaller the particle size, the larger the emission energy; the better the particle-size homogeneity, the narrower the spectral width. The large

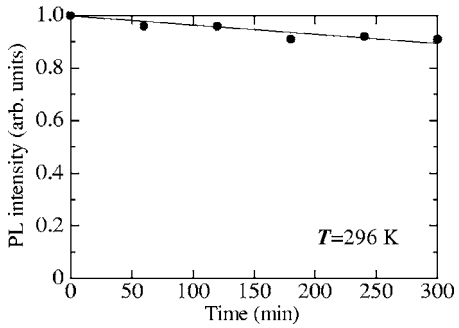

FIG. 5. Long-term behavior of PL intensity of NaF-prepared PSi stored in room ambient.

inner surface area of PSi leads to the proposal that it is largely involved in luminescence. Indeed, surface oxide reduces surface recombination velocity.[33] Surface recombination velocity may be the only parameter required for characterizing the surface;[34] minority carriers produced by photoexcitation are annihilated on the surface by recombination via surface states. The higher the surface recombination velocity the smaller the degree of minority carrier accumulation, or equivalently, the higher the surface recombination velocity the lower the PL intensity. Note that a change in the degree of surface passivation, as well as in that of dielectric effects, can induce wavelength shifts.[2]

As mentioned in Sec. III B, however, no detailed particle-size evaluation was performed in this study. Also, the reason the aqueous NaF (KF) solution can enable the production of such fine-structured materials is not clear at present. Further study is, thus, needed to clarify the origin of ~3.3 eV emission in alkali-fluoride-prepared PSi samples.

Owing to its unstable structure, a porous material is subject to a significant evolution with time, which can directly affect its luminescent properties. Because of its technological importance, the stability of luminescence efficiency has been extensively investigated.[35–43] Finally, we show in Fig. 5 the long-term behavior of the PL intensity of NaF-prepared PSi stored in room ambient. A slight degradation in the PL intensity can be recognized in Fig. 5, suggesting a slight change in the chemical/physical properties of the PSi surface. We also understand that our PSi sample is more stable than hydrogen-passivated anodic PSi, but is less stable than oxygen-stabilized PSi.[38]

CONCLUSIONS

We have shown that photosynthesized PSi in aqueous NaF (KF) solution can emit light in the UV region at room temperature. The observed PL spectra exhibited a peak at ~3.3 eV with a FWHM of ~0.1 eV. The corresponding spectra were clearly different from those observed in silicon oxide (silica) and silicon nanostructures. It was considered that quantum confinement and surface passivation effects enable the observation of stable UV emission at ~3.3 eV. Further study is needed to clarify the microstructure and UV emission mechanism in such unique UV-emitting PSi samples.

[1] A. G. Cullis, L. T. Canham, and P. D. J. Calcott, J. Appl. Phys. **82**, 909 (1997).
[2] S. Ossicini, L. Pavesi, and F. Priolo, *Light Emitting Silicon for Microphotonics* (Springer, Berlin, 2003).
[3] R. W. Fathauer, T. George, A. Ksendzov, and R. P. Vasquez, Appl. Phys. Lett. **60**, 995 (1992).
[4] S. Shih, K. H. Jung, T. Y. Hsieh, J. Sarathy, J. C. Campbell, and D. L. Kwong, Appl. Phys. Lett. **60**, 1863 (1992).
[5] W. B. Dubbelday, D. M. Szaflarski, R. L. Shimabukuro, and S. D. Russell, Appl. Phys. Lett. **62**, 1694 (1993).
[6] J. L. Coffer, S. C. Lilley, R. A. Martin, and L. A. Files-Sesler, J. Appl. Phys. **74**, 2094 (1993).
[7] M. J. Winton, S. D. Russell, J. A. Wolk, and R. Gronsky, Appl. Phys. Lett. **69**, 4026 (1996).
[8] N. Noguchi and I. Suemune, Appl. Phys. Lett. **62**, 1429 (1993).
[9] O. K. Andersen, T. Frello, and E. Veje, J. Appl. Phys. **78**, 6189 (1995).
[10] N. Yamamoto, A. Sumiya, and H. Takai, Mater. Sci. Eng., B **69–70**, 205 (2000).
[11] N. Yamamoto and H. Takai, Thin Solid Films **388**, 138 (2001).
[12] N. Tomita and S. Adachi, Jpn. J. Appl. Phys., Part 1 **40**, 6705 (2001).
[13] H. Noguchi and S. Adachi, Appl. Surf. Sci. **246**, 139 (2005).
[14] K. Tomioka and S. Adachi, Appl. Phys. Lett. **87**, 251920 (2005).
[15] X. Yang, X. L. Wu, S. H. Li, H. Li, T. Qin, Y. M. Yang, P. K. Chu, and G. G. Siu, Appl. Phys. Lett. **86**, 201906 (2005).
[16] G. G. Qin, J. Lin, J. Q. Duan, and G. Q. Yao, Appl. Phys. Lett. **69**, 1689 (1996).
[17] H. Mizuno, H. Koyama, and N. Koshida, Appl. Phys. Lett. **69**, 3779 (1996).
[18] M. V. Wolkin, J. Jorne, P. M. Fauchet, G. Allan, and C. Delerue, Phys. Rev. Lett. **82**, 197 (1999).
[19] Q. Chen, D. L. Zhu, and Y. H. Zhang, Appl. Phys. Lett. **77**, 854 (2000).
[20] E. Hartmann, P. O. Hahn, and R. J. Behm, J. Appl. Phys. **69**, 4273 (1991).
[21] P. N. Vinod and M. Lal, J. Mater. Sci.: Mater. Electron. **16**, 1 (2005).
[22] A. G. Cullis and L. T. Canham, Nature (London) **353**, 335 (1991).
[23] T. George, M. S. Anderson, W. T. Pike, T. L. Lin, R. W. Fathauer, K. H. Jung, and D. L. Kwong, Appl. Phys. Lett. **60**, 2359 (1992).
[24] D. J. Riley, in *Fundamental Electrochemistry and Physics* Semiconductor Micromachining Vol. 1, edited by S. A. Campbell and H. J. Lewerenz (Wiley, Chichester, 1998), p. 277.
[25] E. D. Palik, O. J. Glembocki, I. Heard, Jr., P. S. Burno, and L. Tenerz, J. Appl. Phys. **70**, 3291 (1991).
[26] S. Adachi, *Group IV Semiconductors*, Handbook on Physical Properties of Semiconductors Vol. 1, (Kluwer Academic, Boston, 2004).
[27] Z. Jichang, W. Jiangen, M. Bilan, Z. Jingbing, and Q. Fenyuan, Infrared Phys. **33**, 381 (1992).
[28] D. B. Mawhinney, J. A. Glass, Jr., and J. T. Yates, Jr., J. Phys. Chem. B **101**, 1202 (1997).
[29] A. C. Dillon, M. B. Robinson, and S. M. George, Surf. Sci. Lett. **295**, L998 (1993).
[30] N. Chiodini, F. Meinardi, F. Morazzoni, A. Paleari, R. Scotti, and D. Di Martino, Appl. Phys. Lett. **76**, 3209 (2000).
[31] B. Yao, H. Shi, X. Zhang, and L. Zhang, Appl. Phys. Lett. **78**, 174 (2001).
[32] N. Yamamoto and H. Takai, Thin Solid Films **359**, 184 (2000).
[33] K. Tsunoda, E. Ohashi, and S. Adachi, J. Appl. Phys. **94**, 5613 (2003).
[34] V. Grivickas, J. A. Tellefsen, and M. Willander, in *Properties of Crystalline Silicon*, EMIS Datareviews Series No. 20, edited by R. Hull (INSPEC, London, 1999), p. 718.
[35] I. M. Chang, S. C. Pan, and Y. F. Chen, Phys. Rev. B **48**, 8747 (1993).
[36] X. Wang, G. Shi, F. L. Zhang, H. J. Chen, W. Wang, P. H. Hao, and X. Y. Hou, Appl. Phys. Lett. **63**, 2363 (1993).
[37] J. T. Lue, K. Y. Lo, S. K. Ma, C. L. Chen, and C. S. Chang, Solid State Commun. **86**, 593 (1993).
[38] P. M. Fauchet, L. Tsybeskov, S. P. Duttagupta, and K. D. Hirschman, Thin Solid Films **297**, 254 (1997).
[39] C. H. Chen and Y. F. Chen, Solid State Commun. **111**, 681 (1999).
[40] L. I. Belogorokhova, A. I. Belogorokhov, S. A. Gavrilov, V. Yu. Timoshenko, P. K. Kashkarov, M. G. Lisachenko, and S. P. Kobeleva, Phys. Status Solidi A **197**, 228 (2003).
[41] M. Fischer, B. Hillerich, and F. Kozlowski, Thin Solid Films **372**, 209 (2000).
[42] K. Y. Suh, Y. S. Kim, S. Y. Park, and H. H. Lee, J. Electrochem. Soc. **148**, C439 (2001).
[43] D. W. Cooke, R. E. Muenchausen, B. L. Bennett, L. G. Jacobsohn, and M. Nastasi, J. Appl. Phys. **96**, 197 (2004).